RESEARCH ARTICLE

Research based on network pharmacology and molecular docking: Anti-aging effects of *Monarda didyma* L. volatile oil on PC12 cells

Jiarui Zheng[1], Wanyu Xie[1], Jiaxin Li[2], Sida Zhang[3], Yingxue Guo[2, *], Xianghong Meng[2, *]

[1]School of Clinical Medicine, [2]School of Basic Medicine, [3]School of Pharmacy, Jiamusi University, Jiamusi, Heilongjiang, China.

Received: August 23, 2025; **accepted:** December 8, 2025.

American *Monarda*, also known as horsemint or bergamot herb, is a perennial herbaceous plant belonging to the genus *Monarda* in the *Lamiaceae* family. American *Monarda* volatile oil is an essential oil extracted from its leaves, stems, and flowers through steam distillation. Current research indicates that *Monarda* volatile oil exhibits significant anti-inflammatory, antimicrobial, and antioxidant activities. Its primary active constituent, thymol, has been demonstrated to improve cognitive function in rats with brain injury. However, fundamental research on the application of this volatile oil in the context of neurological aging remains notably limited, and its mechanisms of action have not been systematically elucidated. This study aimed to systematically investigate the potential and mechanisms of *Monarda* volatile oil in counteracting neurological aging from a holistic "multi-component, multi-target, multi-pathway" perspective to experimentally validate and investigate the anti-aging effects of *Monarda didyma* L. volatile oil (MDVO) on the nervous system and explore the underlying mechanisms through network pharmacology and molecular docking. The 1,1-diphenyl-2-picrylhydrazyl (DPPH) free radical scavenging, superoxide dismutase (SOD)/glutathione peroxidase (GSH-Px) activity, and inflammatory factors (TNF-α/IL-6) were measured to assess MDVO's antioxidant and anti-inflammatory capabilities, suggesting that MDVO might exert its anti-aging effect by modulating these targets and pathways. MDVO exhibited superior DPPH scavenging ability compared to ascorbic acid (Vc). MDVO increased SOD and GSH-Px activity and reduced malondialdehyde (MDA) and inflammatory factor levels. The results suggested that MDVO might improve nervous system aging through multiple components, targets, and pathways.

Keywords: *Monarda didyma* L. volatile oil; anti-aging; network pharmacology; molecular docking.

[*]**Corresponding authors:** Yingxue Guo and Xianghong Meng, School of Basic Medicine, Jiamusi University, Jiamusi, Heilongjiang 154007, China. Email: guoyx@jmsu.edu.cn (Guo Y), xh5562@sina.com (Meng X).

Introduction

The accelerating global aging population has significantly increased the incidence of neurodegenerative diseases. Individual aging, identified as a key risk factor, has been shown to drive the onset of such conditions through mechanisms like cellular senescence [1]. Identifying effective interventions to slow the aging process is crucial for preventing and managing neurodegenerative disorders. Aging is influenced by multiple factors including genetics, oxidative stress, inflammation, and apoptosis [2]. Among the mechanisms of aging, oxidative stress and inflammation are the most widely studied. These processes induce cellular senescence and accelerate degenerative changes in multiple organs such as skeletal muscle atrophy and

vascular calcification [3, 4], representing core pathological features of aging. Reactive oxygen species (ROS) are oxygen-containing molecules that regulate cellular signaling under physiological conditions. When ROS production exceeds the capacity of the antioxidant system, oxidative stress occurs, disrupting signaling pathways and promoting the release of pro-inflammatory factors [5]. Oxidative stress also triggers the accumulation of metabolic waste, further inducing inflammatory responses [6]. In turn, the inflammatory cascade amplifies extracellular ROS accumulation through the senescence-associated secretory phenotype (SASP), while excessive oxidative stress activates inflammatory pathways such as NF-κB, forming a positive feedback loop that ultimately drives cellular senescence [7].

In the context of nervous system aging, the core mechanisms involve oxidative stress, inflammatory responses, and dysregulated apoptotic pathways [7-9]. As a highly oxygen-consuming organ, the brain has significantly lower antioxidant capacity compared to peripheral tissues such as reduced superoxide dismutase (SOD) and glutathione peroxidase (GSH-Px) activity [10], making it more vulnerable to oxidative damage and accelerated aging, which increases the risk of neurodegenerative diseases like Alzheimer's disease (AD) and Parkinson's disease (PD) [11]. Targeting oxidative stress and inflammation may delay aging-related pathology in neurodegenerative diseases. For example, memantine, an N-methyl-D-aspartate (NMDA) receptor antagonist, selectively inhibits pathological neuronal excitation and reduces the toxicity of Aβ oligomers [12], improving cognitive function in AD patients [13]. However, long-term use may cause side effects such as headaches and drowsiness [14, 15]. Natural plant-derived active compounds, such as resveratrol and curcumin [16, 17], exert anti-aging effects through multi-target mechanisms including activating antioxidant enzymes and scavenging ROS [18], and mimicking caloric restriction to inhibit mechanistic target of rapamycin (mTOR) signaling [19]. These compounds have demonstrated a high safety profile in animal and clinical studies [20], although curcumin carries a risk of elevated liver enzymes and requires nano-carrier technologies to improve its applicability [21]. In contrast, no hepatotoxicity has been reported for *Monarda didyma* L. volatile oil (MDVO), making it a potentially safer alternative. *Monarda didyma* L., a medicinal plant from the *Lamiaceae* family native to North America, contains volatile oil extracts with demonstrated anti-inflammatory, antimicrobial, and free radical-scavenging activities [22]. However, studies on its neuroprotective and anti-aging effects remain limited, particularly in the context of oxidative stress-induced neurodegenerative diseases, and its efficacy has not been systematically validated. PC12 cells, a differentiated rat adrenal medulla pheochromocytoma cell line, are an ideal model for neurological research due to their expression of norepinephrine/dopamine synthesis systems and AD-related neurotransmitter receptors [23, 24], as well as their high sensitivity to neurotoxins such as H_2O_2, amyloid beta (Aβ), and 6-hydroxydopamine (6-OHDA) [25, 26]. These cells are widely used in studies on neuronal injury mechanisms, drug intervention evaluation [27, 28], and modeling of neurodegenerative diseases like AD, PD, and amyotrophic lateral sclerosis (ALS) [26, 29, 30].

This study aimed to investigate the potential of MDVO in mitigating aging-related damage in PC12 cells with a focus on elucidating the senescence-associated signaling pathways it modulated. The research combined network pharmacology predictions with molecular docking validation to explore the anti-aging effects of MDVO on PC12 cells and to identify the key signaling pathways involved. By systematically investigating the multi-component, multi-target, and multi-pathway mechanisms of MDVO, this research addressed a critical gap in understanding its neuroprotective potential. The findings of this research provided new targets and naturally derived therapeutic strategies for combating neurological aging and neurodegenerative diseases, as well as a

theoretical basis for developing neuroprotective strategies based on natural products.

Materials and methods

Cell treatment and 3-(4,5-dimethylthiazol-2-yl)-2,5-diphenyltetrazolium bromide (MTT) assay

MDVO was extracted by our research group using steam distillation. Cryopreserved rat adrenal pheochromocytoma PC12 cells (Procell Life Science & Technology Co., Ltd., Wuhan, Hubei, China) were quickly thawed in a 37°C water bath and immediately transferred to ice followed by resuspending in RPMI-1640 medium (Thermo Fisher Scientific, Waltham, MA, USA) supplemented with 10% FBS and 100 U/mL penicillin under sterile conditions in a biosafety cabinet. After centrifugation at 1,200 ×g for 5 minutes, the cell pellet was resuspended and cultured in a 37°C, 5% CO_2 incubator (Shanghai Lishen Scientific Instrument, Shanghai, China). The cells were passaged when cell confluence reached ≥ 80% at a 1:3 ratio using 0.25% trypsin. Morphological changes were observed and recorded daily. Third-passage cells in the logarithmic growth phase were seeded in 96-well plates at a density of 1×10^4 cells per well and treated with 15 mg/mL D-galactose or varying concentrations of 0 to 100 mg/L MDVO. Cell viability was assessed using the MTT assay, and the MDVO concentrations maintaining viability above 50% were selected as effective doses for subsequent experiments. Cells in each group were cultured for 24, 48, and 72 hours after addition of MDVO. After adding 20 µL of MTT solution to each well, the incubation continued for 4 hours. The medium was discarded, and 150 µL of dimethyl sulfoxide (DMSO) (Biotopped, Beijing, China) was added to each well to dissolve the formazan crystals by shaking. The OD value was measured at 570 nm and repeated three times and averaged. Cell proliferation rate was then calculated as follows.

$$\text{Proliferation rate} = (OD_{\text{experimental group}} - OD_{\text{blank group}}) / (OD_{\text{control group}} - OD_{\text{blank group}}) \times 100\%$$

Determination of antioxidant activity of MDVO

The 1,1-diphenyl-2-picrylhydrazyl (DPPH) radical scavenging capacity was measured according to the method reported by Li *et al*. [31]. Briefly, 100 µL of DPPH solution (Vicqi Biological Technology Co., Ltd., Chengdu, Sichuan, China) was added to a 96-well plate followed by adding 100 µL of the MDVO sample. After thorough mixing, the plate was incubated in the dark at 37℃ for 30 minutes. The absorbance was measured at 519 nm using a microplate reader (Thermo Fisher Scientific, Waltham, MA, USA). Each sample was tested in triplicate and averaged. Vitamin C (Vc) was used as positive control.

Detection of oxidative stress-related indicators

PC12 cells were digested with 0.02% EDTA and collected before they were fully lysed with Radioimmunoprecipitation assay (RIPA) lysis buffer (Beyotime, Shanghai, China), centrifuged at 1,500 xg for 5 minutes at 4°C, and collected the supernatant. SOD enzyme activity was measured using the WST-1 method (Beyotime, Shanghai, China) following manufacturer's instruction. After incubation at 37°C for 20 min, absorbance was measured at 450 nm to calculate the SOD inhibition rate. Malondialdehyde (MDA) content was determined using the thiobarbituric acid (TBA) method (Beyotime, Shanghai, China) following manufacturer's instruction. MDA levels were quantified by measuring absorbance at 532 nm. GSH-Px activity was assayed by measuring its ability to catalyze the H_2O_2-dependent oxidation of reduced glutathione (GSH) to oxidized glutathione (GSSG) using a micro-method kit (Solarbio, Beijing, China) following the manufacturer's instruction. The enzyme activity was calculated based on the change in absorbance at 412 nm. GSH-Px activity was expressed in units (U), defined as the amount of enzyme that catalyzed the oxidation of 1 nmol of GSH per minute per gram of sample.

Detection of inflammation-related indicators

The levels of inflammatory indicators IL-1β, TNF-α, and IL-6 were detected using enzyme-linked immunosorbent assay (ELISA) kit (Enzyme-linked

Biotechnology, Shanghai, China) following manufacturer's instruction.

Collection of bioactive compounds and gene targets of MDVO

MDVO sample was analyzed through gas chromatography – mass spectrometry (GC-MS) (Agilent Technologies, Santa Clara, CA, USA) using DB-1 capillary column (0.25 mm × 60 m, 0.25 µm), N_2 (99.999%) as carrier gas, 1 mL/min flow rate, 250°C injector temperature, 40:1 split ratio, and 2 µL injection volume. Temperature was programed as initial 60°C for 4 min, ramp at 3°C/min to 150°C for 10 min, then ramp at 10°C/min to 240°C for 10 min. Electron ionization (EI) was 230°C, and electron energy was 70 eV. The interface temperature was 280°C with solvent delay of 7.5 min, mass range (m/z) of 33 - 350, and multiplier voltage of 2.4 kV. The screened compounds were searched for their Simplified Molecular Input Line Entry System (SMILES) numbers in the PubChem database (https://pubchem.ncbi.nlm.nih.gov/), and then input into the SuperPred (https://prediction.charite.de/) and SwissTargetPrediction (http://www.swisstargetprediction.ch/) databases to predict the targets of each potential component.

Collection of overlapping targets related to MDVO, aging, and antioxidant effects

Targets were retrieved by using the keywords of "aging" and "oxidative stress-related neurodegenerative diseases (OSND)" from Online Mendelian Inheritance in Man (OMIM) (https://omim.org/) and GeneCards (https://www.genecards.org/). Data retrieval was up to July 2025. Disease genes related to the two keywords were downloaded from the databases. Subsequently, the target lists were combined, and any duplicate targets were removed to create a list of targets related to aging and antioxidant effects. The overlap between drug-related and disease-related genes was visualized using Venny diagram (https://bioinfogp.cnb.csic.es/tools/venny/).

Construction of herb-component-disease-target network

Cytoscape 3.10.1 (https://cytoscape.org/) was used to construct the "Drug-Component-Disease-Target" network. In this network, components and targets were represented as different graphical nodes, and the interconnections between them were represented by edges. The intersection targets identified by Venny analysis were imported into the STRING database (http://string-db.org/) to predict protein-protein interaction (PPI) relationships among them. The PPI data was then imported into Cytoscape for visualization. The CytoHubba, a plugin for Cytoscape, was used to calculate network topological features and construct the PPI network. Cytoscape 3.10.1 was used to draw and visualize the network analysis.

Gene ontology (GO) functional and Kyoto encyclopedia of genes and genomes (KEGG) pathway enrichment analysis

The database for annotation, visualization and integrated discovery (DAVID) (http://david.abcc.ncifcrf.gov/) was used to analyze the functional and pathway enrichment of the differential genes. Potential targets obtained from GO (http://www.bioinformatics.com.cn/) functional annotation were analyzed online and imported into DAVID, which included potential targets and their associated signaling pathways (KEGG) (http://www.bioinformatics.com.cn/). The enrichment results were then visualized using bubble plots generated with a bioinformatics platform (https://www.bioinformatics.com.cn/).

Molecular docking

The 3D structures of the top 5 most abundant compounds were downloaded from the PubChem database on March 12, 2025. The structures of 12 relevant receptor proteins were downloaded from the PDB database (https://www.rcsb.org/). PyMOL software (v 2.6) (https://pymol.org/) was used for hydrogen removal and water addition. AutoDock (v 1.5.6) (https://autodocksuite.scripps.edu/adt/) was used to prepare the files and conduct molecular docking. Visualization was done using PyMOL. Binding energy scores were extracted and ranked.

Statistical analysis

SPSS (v 27) (IBM, Armonk, New York, USA) was employed for statistical analysis. Data were measured at least three times and expressed as mean ± standard deviation. Statistical differences were evaluated using analysis of variance (ANOVA) with the *P* value less than 0.05, 0.01, and 0.001 as the statistically significant, highly significant, and extremely significant differences, respectively.

Results and discussion

Antioxidant activity of MDVO

The results showed that the free radical scavenging and reducing capacities of MDVO were positively correlated with concentration. Compared to Vc, MDVO exhibited superior DPPH radical scavenging ability (Figure 1).

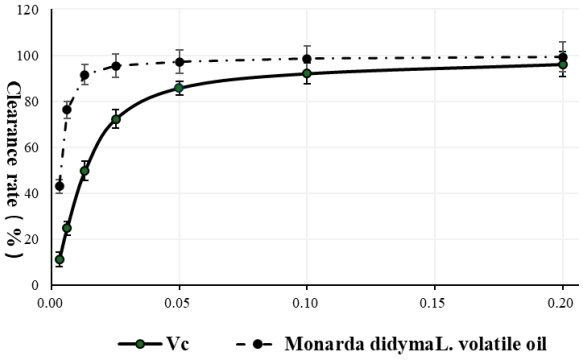

Figure 1. DPPH radical scavenging rate of MDVO and Vc.

Effect of MDVO on proliferation of d-gal-induced PC12 cells

Within the concentration range from 0 to 100 mg/L, the proliferation viability of D-gal-induced PC12 cells increased with increasing concentration of MDVO. When the MDVO concentration exceeded 12.5 mg/L, the 24-hour proliferation rate of cells in both control and experimental groups was above 50%. Therefore, concentrations of 12.5, 25, and 50 mg/L were selected as the gradient working concentrations for MDVO and defined as oil-L, oil-M, and oil-H, respectively (Figure 2).

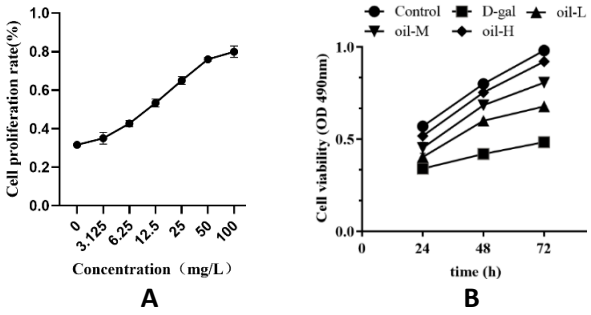

Figure 2. Comparison of D-gal-induced PC12 cell proliferation viability. **A.** under different concentrations of MDVO. **B.** among different MDVO concentration groups.

Effect of MDVO on oxidative stress in d-gal-induced PC12 cells

SOD and GSH-Px are the main antioxidant enzymes in the body, commonly used to assess the body's antioxidant capacity. MDA is a product of lipid peroxidation, and its levels reflect the extent of oxidative damage. The comparative analysis results showed that, after D-gal treatment, SOD and GSH-Px enzyme activities of PC12 cells significantly decreased, while MDA content significantly increased ($P < 0.05$). After adding MDVO, SOD and GSH-Px enzyme activities increased to varying degrees in each group, while MDA content decreased to varying degrees ($P < 0.05$). The results demonstrated that the changes in the different MDVO concentration groups were dose-dependent and therefore suggested that MDVO could alleviate oxidative stress in senescent cells to a certain extent, thereby ameliorating senescence (Table 1).

Table 1. Comparison of oxidative stress indicators in PC12 cells among different groups.

Group	SOD (U/mL)	GSH-px (U/mL)	MDA (μmol/L)
control	32.46 ± 1.26	25.46 ± 1.17	5.13 ± 0.82
D-gal	13.37 ± 1.20*	10.33 ± 1.24*	16.32 ± 1.31*
oil-L	16.64 ± 1.06#	15.42 ± 1.21#	13.66 ± 0.95#
oil-M	20.49 ± 1.59#	21.33 ± 1.64#	10.38 ± 0.64#
oil-H	28.35 ± 1.23#	24.18 ± 1.32#	6.54 ± 1.16#

Note: *: $P < 0.05$ compared with control group. #: $P < 0.05$ compared with D-gal group.

Effect of MDVO on inflammation in d-gal-induced PC12 cells

Results of inflammatory cytokine detection showed that the levels of IL-1β, IL-6, and TNF-α were significantly elevated in cells after D-gal treatment ($P < 0.05$). However, after adding MDVO, the levels of IL-1β, TNF-α, and IL-6 showed a decreasing trend in each group. Furthermore, the levels of inflammatory cytokines in different MDVO concentration groups decreased sequentially with increasing MDVO concentrations (Table 2).

Table 2. Comparison of inflammatory indicators in PC12 cells among different groups.

Group	IL-1β (pg/mL)	IL-6 (pg/mL)	TNF-α (μg/L)
control	2.63 ± 0.58	1.78 ± 0.36	1.52 ± 0.33
D-gal	9.32 ± 0.87*	6.85 ± 0.82*	8.44 ± 0.51*
oil-L	8.06 ± 0.53	5.62 ± 0.60	6.05 ± 0.28#
oil-M	5.93 ± 0.56#	4.35 ± 0.46#	4.28 ± 0.31#
oil-H	3.62 ± 0.42#	2.71 ± 0.40#	3.11 ± 0.21#

Note: *: $P < 0.05$ compared with control group. #: $P < 0.05$ compared with D-gal group.

Collection of MDVO active components

Seven (7) active compounds in MDVO were identified, which included 2-thujene, α-pinene, myrcene, terpinolene, o-cymene, γ-terpinene, and thymol. The canonical SMILES, chemical formula, molecular weight, and PubChem ID for these 7 compounds were downloaded from PubChem. The SuperPred platform was used to predict targets for each compound. All predicted targets were then merged using Excel by removing duplicates, resulting in a total of 236 related targets.

Disease target gene prediction

Gene targets matched the keywords of "anti-aging" and "oxidative stress-related neurodegenerative diseases (OSND)" were collected from the GeneCards and OMIM databases. By matching 89 drug targets and 3,649 disease targets, 87 common targets were identified as the potential candidates for MDVO in ameliorating related diseases (Figure 3A). An "Active Component-Therapeutic Target" network was then constructed to further identify the key molecular mechanisms involving 7 components and 48 potential targets. All seven active components interacted with ≥ 3 aging-related targets (Figure 3B). The results indicated that MDVO and its components might affect multiple targets, leading to complex pharmacological changes and comprehensive overall effects.

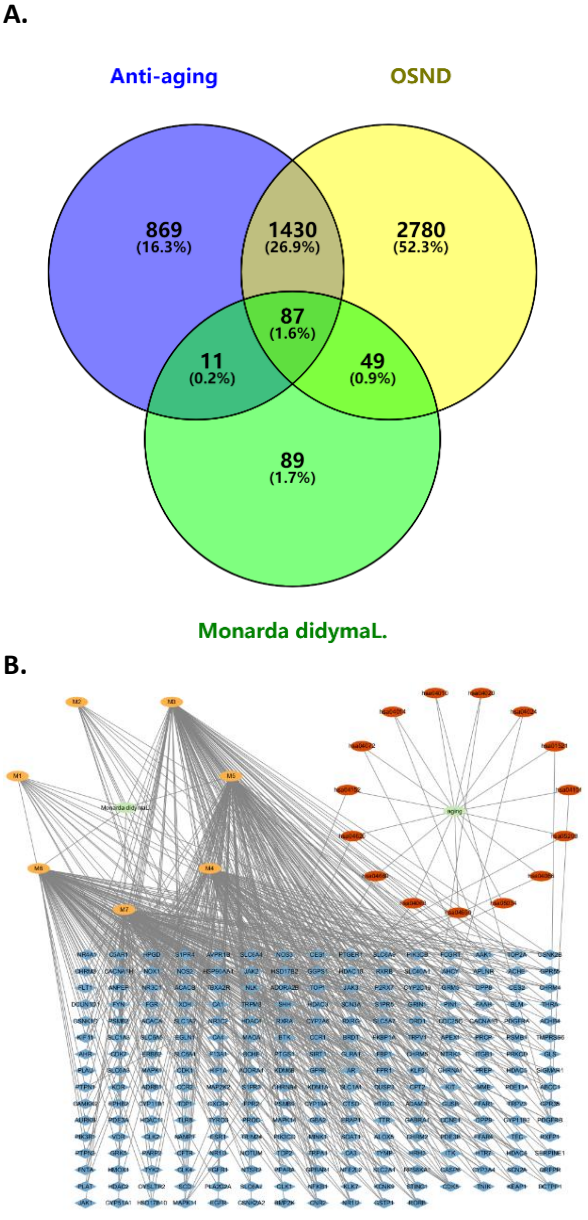

Figure 3. Network pharmacology analysis of MDVO for antioxidant and anti-aging effects. **A.** Venn diagram of drug-disease common targets (87 intersection targets). **B.** Drug-component-disease-target network diagram. Orange represented components. Red represented pathways. Blue represented genes. Green represented drug (left) and disease (right), respectively.

Table3. Topology analysis of core targets in the PPI network.

Gene	Degree	Betweenness centrality	Closeness centrality
HSP90AA1	74	0.110829152	0.551807228
EGFR	73	0.110023352	0.564039408
ESR1	68	0.106769230	0.547846889
HIF1A	61	0.067079503	0.510022271
NFKB1	57	0.040069879	0.522831050
ERBB2	51	0.034311733	0.497826086
SIRT1	49	0.038101648	0.496746203
PPARA	42	0.046700001	0.485169491
KDR	40	0.023847886	0.471193415
JAK2	38	0.033362683	0.476091476
MAPK1	37	0.017348374	0.470225872
MAPK14	37	0.011823105	0.465447154

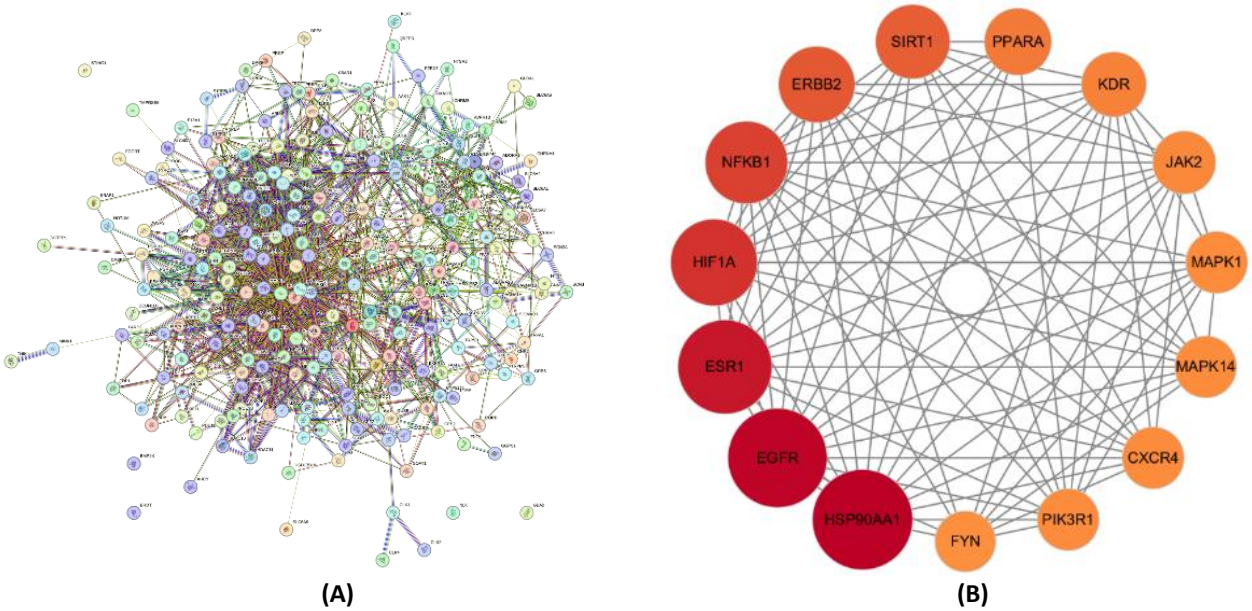

Figure 4. PPI protein-protein interaction network diagram (**A**) and core targets related to MDVO's antioxidant and anti-aging effects (**B**).

Protein-protein interaction (PPI) network construction and analysis

To explore the mechanism of active components in MDVO for anti-aging and antioxidant effects, a protein-protein interaction (PPI) network was constructed by inputting 32 targets into the STRING database (Figure 4A). The topological analysis of the PPI network resulted that the top 12 targets were selected as important targets influencing anti-aging and antioxidant effects with a degree of regulation greater than 10 (Table 3), serving as receptor proteins for subsequent molecular docking (Figure 4B).

Gene ontology (GO) and Kyoto encyclopedia of genes and genomes (KEGG) pathway enrichment

GO pathway enrichment analysis screened the top 10 terms for biological process (BP), cellular component (CC), and molecular function (MF). BP mainly included chemical synaptic transmission, insulin-like growth factor receptor

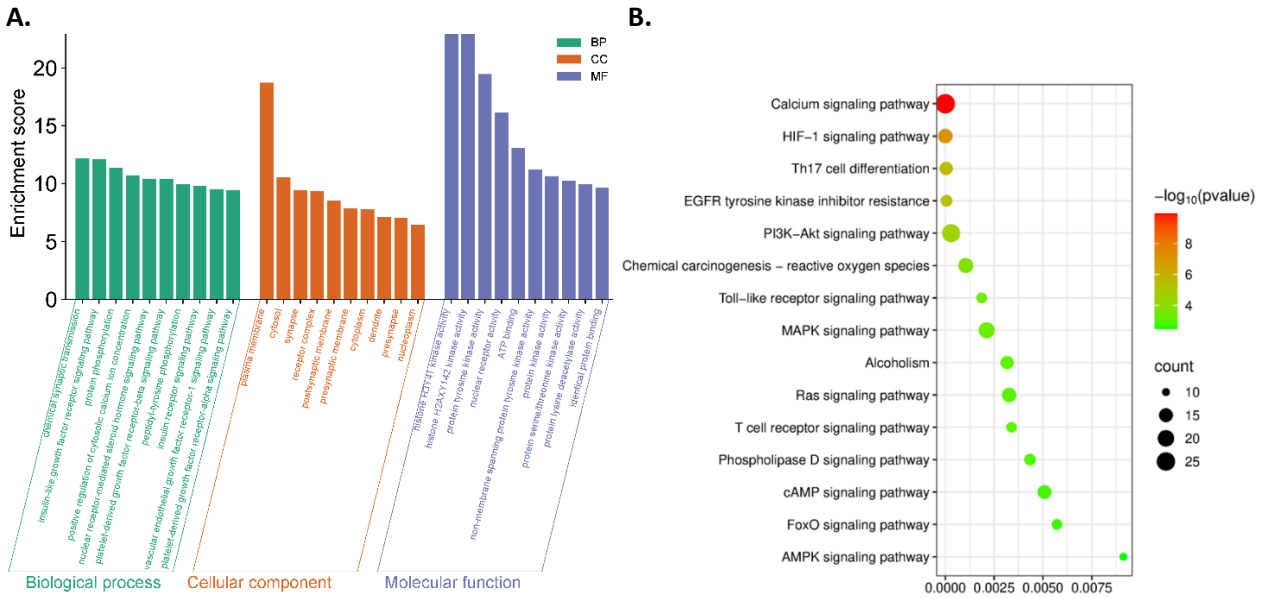

Figure 5. GO (**A**) and KEGG pathway (**B**) enrichment analysis.

signaling pathway, protein phosphorylation, positive regulation of cytosolic calcium ion concentration, nuclear receptor-mediated steroid hormone signaling pathway, platelet-derived growth factor receptor-beta signaling pathway, protein tyrosine phosphorylation, insulin receptor signaling pathway, vascular endothelial growth factor receptor-1 signaling pathway, platelet-derived growth factor receptor-alpha signaling pathway. CC included plasma membrane, cytosol, synapse, receptor complex, postsynaptic membrane, presynaptic membrane, cytoplasm, dendrite, presynaptic active zone, nucleoplasm. MF included histone H3-Y41 kinase activity, histone H2A-X-Y142 kinase activity, protein tyrosine kinase activity, nuclear receptor activity, ATP binding, non-membrane spanning protein tyrosine kinase activity, protein kinase activity, protein serine/threonine kinase activity, protein lysine deacetylase activity, identical protein binding (Figure 5A). KEGG pathway analysis revealed pathways including calcium signaling pathway, HIF-1 signaling pathway, Th17 cell differentiation, EGFR tyrosine kinase inhibitor resistance, PI3K-Akt signaling pathway, chemical carcinogenesis-reactive oxygen species, toll-like receptor signaling pathway, MAPK signaling pathway, regulation of alcohol dependence, Ras signaling pathway, T cell receptor signaling pathway, phospholipase D signaling pathway, cAMP signaling pathway, FoxO signaling pathway, AMPK signaling pathway. GO and KEGG enrichment analysis showed that the MAPK pathway was not only significantly enriched but also associated with a large number of genes. The biological processes that it regulates such as anti-apoptosis and anti-inflammation are directly related to the improvement of antioxidant and anti-aging effects. Kong *et al*. demonstrated that icariin inhibited TNF-α/IFN-γ-induced inflammatory response in HaCaT cells by suppressing the p38 MAPK signaling pathway [32]. Activation of the MAPK signaling pathway could promote senescence in HS-1 skin cancer cells by affecting the expression of senescence markers p53/p21 [33], which suggested that the MAPK pathway might be the primary route through which MDVO regulated oxidative stress and aging. Further, the chemical carcinogenesis - reactive oxygen species pathway was primarily triggered by ROS and could activate signaling pathways such as MAPK, NF-κB, and PI3K-Akt, regulating cell proliferation, differentiation, and apoptosis (Figure 5B).

Table 4. Molecular docking binding energies.

	Thymol	γ-Terpinene	o-Cymene	Terpinolene	Myrcene
HSP90AA1	-4.04	-4.29	-3.23	-4.16	-3.93
EGFR	-5.40	-5.55	-4.91	-3.50	-4.84
ESR1	-5.07	-5.75	-4.90	-5.14	-5.08
HIF1A	-5.48	-5.32	-4.28	-4.72	-4.60
NFκB	-4.54	-5.28	-3.56	-4.48	-4.24
ERBB2	-4.46	-4.21	-3.31	-4.03	-3.87
SIRT1	-5.48	-5.61	-4.87	-5.11	-5.12
PPARA	-5.79	-6.04	-5.30	-6.03	-5.57
KDR	-5.14	-5.65	-4.66	-5.13	-5.05
JAK2	-5.11	-5.14	-4.29	-4.65	-4.65
MAPK1	-4.74	-5.06	-3.74	-4.53	-4.12
MAPK14	-5.65	-5.56	-4.56	-5.04	-5.07

Molecular docking

Molecular docking was performed to evaluate the binding affinity of obtained target small molecules and proteins. Binding energy (kcal/mol) was determined through docking analysis for the prediction of the binding ability of active compounds to their targets. Lower scores indicated stronger binding affinity, meaning the compound bound more tightly to the target. A binding energy less than -5 kcal/mol was generally considered to indicate relatively stable binding. Docking results for the top 12 genes revealed that the MAPK pathway frequently cross-regulated with other signaling nodes (Table 4). EGFR was an upstream activator of the MAPK/ERK pathway. Binding EGFR to its ligand EGF could activate downstream pathways like Ras/Raf/MAPK and PI3K/Akt [34]. The MAPK pathway could phosphorylate and activate NF-κB, mediating inflammatory responses. TNF-α, IL-6, and IL-1β have been confirmed as downstream effector molecules of the MAPK/NF-κB pathway [35]. Thymol showed stable binding affinity for PPARA and MAPK, which might function by regulating the MAPK pathway, particularly MAPK14 (p38 MAPK), playing a key role in inflammatory and oxidative stress responses. γ-terpinene exhibited stable binding to most core targets. o-cymene showed stable binding to PPARA that played a role in lipid metabolism and inflammatory responses [36], which made it an important target for thymol, thereby enhancing the anti-inflammatory and antioxidant effects of MDVO. The results indicated that the antioxidant and anti-aging effects of MDVO were primarily mediated by thymol, γ-terpinene, and o-cymene as the main active components. Therefore, the mechanism by which MDVO delayed aging might involve multiple pathways (Figure 6).

MDVO demonstrated potential in regulating neurological aging with its DPPH radical scavenging capacity significantly superior to ascorbic acid (Vc) and effectively enhancing the activity of antioxidant enzymes SOD and GSH-Px while simultaneously reducing MDA and inflammatory cytokine TNF-α and IL-6 levels, confirming its therapeutic value in ameliorating neurological aging. Network pharmacology and molecular docking results indicated that MDVO's core active components thymol and γ-terpinene strongly bound to key targets MAPK14 (p38α) and PPARA. Multiple targets synergistically regulated aging through interactions of oxidative stress by activating the Nrf2/HO-1 pathway and inflammatory response by inhibiting the NF-κB pathway. Core pathway interactions revealed the p38 MAPK-Nrf2 axis with p38 MAPK (MAPK14) directly phosphorylating Nrf2, therefore, negative feedback inhibiting its antioxidant function [37, 38]. MDVO antagonized this effect and released Nrf2 inhibition. The MAPK/NF-κB inflammatory cascade demonstrated that MAPK activation drove NF-κB nuclear translocation,

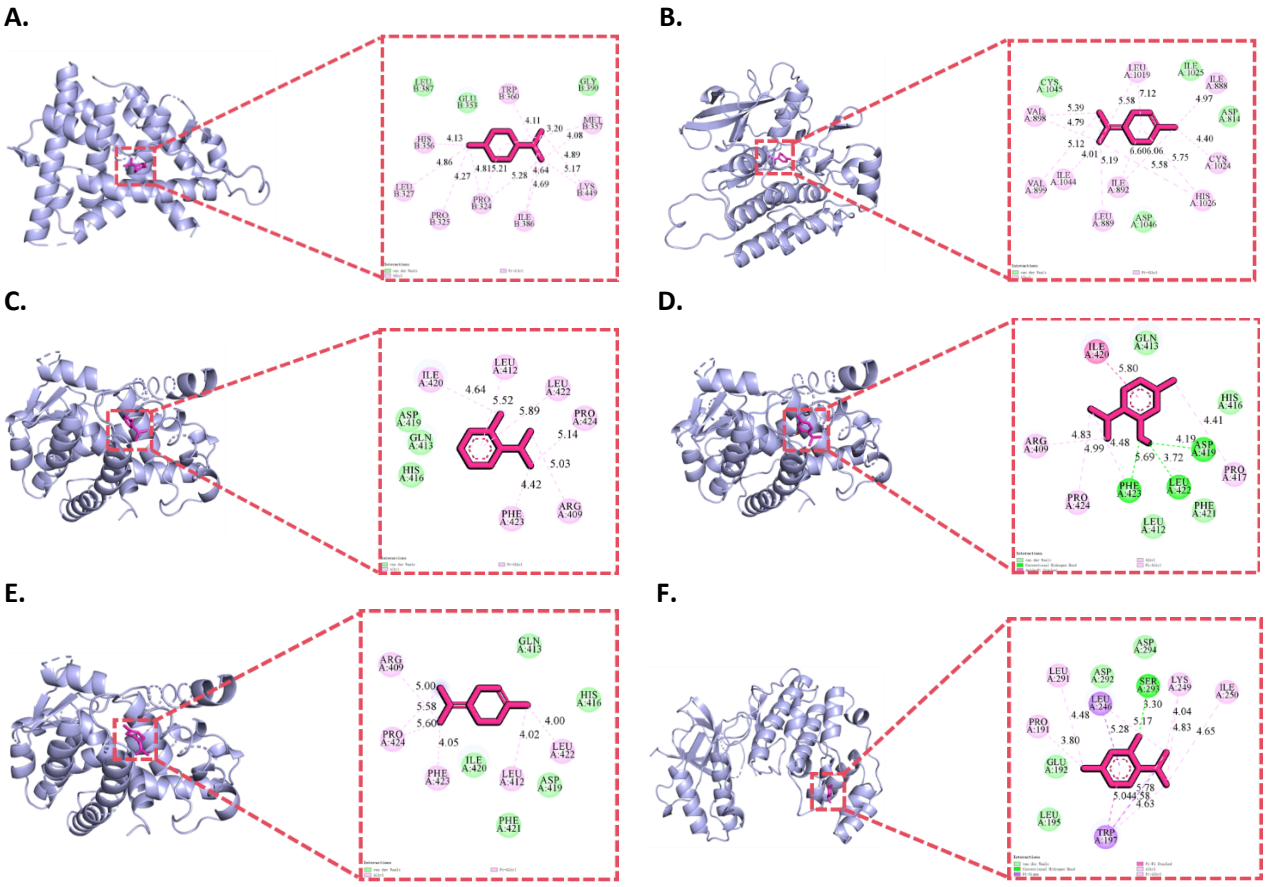

Figure 6. Molecular docking diagrams with 2D and 3D plots. A. γ-terpinene-ESR1. B. γ-terpinene-KDR. C. o-cymene-PPARA. D. thymol-PPARA. E. γ-terpinene-PPARA. F. thymol-MAPK14. ESR1: estrogen receptor 1. KDR: kinase insert domain receptor (VEGFR2). PPARA: peroxisome proliferator activated receptor alpha. MAPK14: Mitogen-activated protein kinase 14 (p38α).

promoted the release of chemokines like MCP-1 [39], and together synergistically induced the senescence-associated secretory phenotype (SASP) in an inflammatory microenvironment [40]. Multi-pathway network integration showed that MDVO formed a regulatory network by simultaneously modulating the MAPK-p38, Nrf2/HO-1, PI3K/AKT, and NF-κB pathways. Within this network, PI3K/AKT enhanced cell survival signaling to antagonize apoptosis, while Nrf2/HO-1 and NF-κB constituted an oxidation-inflammation balance axis. MDVO broke the oxidative stress-inflammation-aging cascade by synergistically regulating the multi-pathway network of MAPK-p38/Nrf2, NF-κB, and PI3K/AKT, providing a theoretical breakthrough for the development of natural-source neuroprotective agents.

Acknowledgements

This study was supported by the Heilongjiang Provincial University Basic Scientific Research Business Fund Project (Grant No. 2023-KYYWF-0588) and the Key Laboratory of Microecology-Immune Regulation Network and Related Diseases, Basic Medical College, Jiamusi University, Jiamusi, Heilongjiang, China.

References

1. Hou Y, Dan X, Babbar M, Wei Y, Hasselbalch SG, Croteau DL, *et al*. 2019. Ageing as a risk factor for neurodegenerative disease. Nat Rev Neurol. 15(10):565-581.
2. Lapierre LR, De Magalhaes Filho CD, McQuary PR, Chu CC, Visvikis O, Chang JT, *et al*. 2013. The TFEB orthologue HLH-30

regulates autophagy and modulates longevity in *Caenorhabditis elegans*. Nat Commun. 4:2267.
3. Chen M, Wang Y, Deng S, Lian Z, Yu K. 2022.Skeletal muscle oxidative stress and inflammation in aging: Focus on antioxidant and anti-inflammatory therapy. Front Cell Dev Biol. 10:964130.
4. Serino A, Salazar G. 2018.Protective role of polyphenols against vascular inflammation, aging and cardiovascular disease. Nutrients. 11(1):53.
5. Demel HR, Feuerecker B, Piontek G, Seidl C, Blechert B, Pickhard A, *et al*. 2015. Effects of topoisomerase inhibitors that induce DNA damage response on glucose metabolism and PI3K/Akt/mTOR signaling in multiple myeloma cells. Am J Cancer Res. 5(5):1649-1664.
6. Zhou NJ, Bao WQ, Zhang CF, Jiang ML, Liang TL, Ma GY, *et al*. 2025. Immunometabolism and oxidative stress: Roles and therapeutic strategies in cancer and aging. NPJ Aging. 11(1):59.
7. Xu X, Pang Y, Fan X. 2025. Mitochondria in oxidative stress, inflammation and aging: From mechanisms to therapeutic advances. Signal Transduct Target Ther. 10(1):190.
8. Niu X, Zheng S, Liu H, Li S. 2018. Protective effects of taurine against inflammation, apoptosis, and oxidative stress in brain injury. Mol Med Rep. 18(5):4516-4522.
9. Wang H, Zhou XM, Wu LY, Liu GJ, Xu WD, Zhang XS, *et al*. 2020. Aucubin alleviates oxidative stress and inflammation *via* Nrf2-mediated signaling activity in experimental traumatic brain injury. J Neuroinflammation. 17(1):188.
10. Cobley JN, Fiorello ML, Bailey DM. 2018. 13 reasons why the brain is susceptible to oxidative stress. Redox Biol. 15:490-503.
11. Stephenson J, Nutma E, van der Valk P, Amor S. 2018. Inflammation in CNS neurodegenerative diseases. Immunology. 154(2):204-219.
12. Kunugi H, Ueki A, Otsuka M, Isse K, Hirasawa H, Kato N, *et al*. 2001. A novel polymorphism of the brain-derived neurotrophic factor (BDNF) gene associated with late-onset Alzheimer's disease. Mol Psychiatry. 6(1):83-86.
13. Forlenza OV, Diniz BS, Teixeira AL, Ojopi EB, Talib LL, Mendonca VA, *et al*. 2010. Effect of brain-derived neurotrophic factor Val66Met polymorphism and serum levels on the progression of mild cognitive impairment. World J Biol Psychiatry. 11(6):774-780.
14. Shafiei-Irannejad V, Abbaszadeh S, Janssen PML, Soraya H. 2021. Memantine and its benefits for cancer, cardiovascular and neurological disorders. Eur J Pharmacol. 910:174455.
15. Stynen B, Abd-Rabbo D, Kowarzyk J, Miller-Fleming L, Aulakh SK, Garneau P, *et al*. 2018. Changes of cell biochemical states are revealed in protein homomeric complex dynamics. 175(5):1418-1429. e9.
16. Jardim FR, de Rossi FT, Nascimento MX, da Silva Barros RG, Borges PA, Prescilio IC, *et al*. 2018. Resveratrol and brain mitochondria: A review. Mol Neurobiol. 55(3):2085-2101.
17. Banji OJ, Banji D, Ch K. 2014. Curcumin and hesperidin improve cognition by suppressing mitochondrial dysfunction and apoptosis induced by D-galactose in rat brain. Food Chem Toxicol. 74:51-59.
18. Shen LR, Xiao F, Yuan P, Chen Y, Gao QK, Parnell LD, *et al.* 2013. Curcumin-supplemented diets increase superoxide dismutase activity and mean lifespan in *Drosophila*. Age (Dordr). 35(4):1133-1142.
19. Lao CD, Demierre MF, Sondak VK. 2006. Targeting events in melanoma carcinogenesis for the prevention of melanoma. Expert Rev Anticancer Ther. 6(11):1559 1568.
20. Chen X, Bahramimehr F, Shahhamzehei N, Fu H, Lin S, Wang H, *et al*. 2024. Anti-aging effects of medicinal plants and their rapid screening using the nematode *Caenorhabditis elegans*. Phytomedicine. 129:155665.
21. Kheiripour N, Plarak A, Heshmati A, Asl SS, Mehri F, Ebadollahi-Natanzi A, *et al*. 2021. Evaluation of the hepatoprotective effects of curcumin and nanocurcumin against paraquat-induced liver injury in rats: Modulation of oxidative stress and Nrf2 pathway. J Biochem Mol Toxicol. 35(5):e22739.
22. Côté H, Pichette A, St-Gelais A, Legault J. 2021. The biological activity of *Monarda didyma* L. essential oil and its effect as a diet supplement in mice and broiler chicken. Molecules. 26(11):3368.
23. Xie D, Deng T, Zhai Z, Sun T, Xu Y. 2023. The cellular model for Alzheimer's disease research: PC12 cells. Front Mol Neurosci. 15:1016559.
24. Westerink RH, Ewing AG. 2008. The PC12 cell as model for neurosecretion. Acta Physiol (Oxf). 192(2):273-285.
25. Zhang C, Yu P, Ma J, Zhu L, Xu A, Zhang J. 2019. Damage and phenotype change in PC12 cells induced by lipopolysaccharide can be inhibited by antioxidants through reduced cytoskeleton protein synthesis. Inflammation. 42(6):2246-2256.
26. Jiang Z, Liu D, Li T, Gai C, Xin D, Zhao Y, *et al*. 2025. Hydrogen sulfide reduces oxidative stress in Huntington's disease *via* Nrf2. Neural Regen Res. 20(6):1776-1788.
27. Zhou T, Mo J, Xu W, Hu Q, Liu H, Fu Y, *et al*. 2023. Mild hypothermia alleviates oxygen-glucose deprivation/reperfusion-induced apoptosis by inhibiting ROS generation, improving mitochondrial dysfunction and regulating DNA damage repair pathway in PC12 cells. Apoptosis. 28(3-4):447-457.
28. Zhang H, Zhou W, Li J, Qiu Z, Wang X, Xu H, *et al*. 2022. Senegenin rescues PC12 cells with oxidative damage through inhibition of ferroptosis. Mol Neurobiol. 59(11):6983-6992.
29. Tan FHP, Ting ACJ, Leow BG, Najimudin N, Watanabe N, Azzam G. 2021. Alleviatory effects of Danshen, Salvianolic acid A and Salvianolic acid B on PC12 neuronal cells and *Drosophila melanogaster* manu of Alzheimer's disease. J Ethnopharmacol. 279:114389.
30. Zhang W, Benmohamed R, Arvanites AC, Morimoto RI, Ferrante RJ, Kirsch DR, *et al*. 2012. Cyclohexane 1,3-diones and their inhibition of mutant SOD1-dependent protein aggregation and toxicity in PC12 cells. Bioorg Med Chem. 20(2):1029-1045.
31. Li X, Lin J, Gao Y, Han W, Chen D. 2012. Antioxidant activity and mechanism of *Rhizoma Cimicifugae*. Chem Cent J. 6(1):140.
32. Kong L, Liu J, Wang J, Luo Q, Zhang H, Liu B, *et al*. 2015. Icariin inhibits TNF-α/IFN-γ induced inflammatory response *via* inhibition of the substance P and p38-MAPK signaling pathway in human keratinocytes. Int Immunopharmacol. 29(2):401-407.
33. Zhao XD, Huang C, Wang RX, Wang SA. 2021. DUSP22 promotes senescence of HS-1 skin cancer cells through triggering MAPK signaling pathway. Eur Rev Med Pharmacol Sci. 25(3):1163.

34. Zhang H, Mao Y, Zou X, Niu J, Jiang J, Chen X, *et al*. 2023. Triptonide inhibits growth and metastasis in HCC by suppressing EGFR/PI3K/AKT signaling. Neoplasma. 70(1):94-102.
35. Arrieta MC, Bistritz L, Meddings JB. 2006. Alterations in intestinal permeability. 55(10):1512-1520.
36. Huang J, Zhou K, Li J, Xu Z, Wu X, Chen T, *et al*. 2025. Poncirin ameliorates alcoholic liver injury by regulating lipid metabolism and inflammatory response in a PPARα dependent manner. Phytomedicine. 140:156598.
37. Berköz M. 2025. Immunomodulation and antioxidant effects of diffractaic acid in LPS-stimulated RAW264.7 cells mediated by the Nrf2/HO-1 and NF-κB signaling pathways. Cell Tiss Biol. 19:458–469.
38. Tan J, Wang D, Dong W, Zhang J, Li Y, Zhao L, *et al*. 2025. CEBPB activates NRF2 to regulate the MAPK pathway through DUSP1 to promote proliferation and antioxidant capacity in ovarian cancer cells. Cell Cycle. 24(5-8):122-140.
39. Epstein MS, Cash BD, Shah S. 2015. Rapid relief of irritable bowel syndrome (IBS) symptoms with targeted delivery of L-menthol to the small intestine: Results from 2 clinical trials and a patient survey: 1746. Am J Gastroenterol. 110:S741.
40. Zhou Y, Xiao J, Peng S, Pang X, Ma D, Gui Y, *et al*. 2025. The integration of link proteomics with transcriptomics elucidates that TNF-α induces senescence and apoptosis in transplanted mesenchymal stem cells. Stem Cell Rev Rep. 21(7):2298-2309.